*Inorg. Chem.* **2006**, *45*, 454–459

# Synthesis, Characterization, and Electrochemical Studies on [1.1]Ferrocenophanes Containing Aluminum, Gallium, and Indium

**Jörg A. Schachner,[†] Grzegorz A. Orlowski,[†] J. Wilson Quail,[§] Heinz-Bernhard Kraatz,[†] and Jens Müller*,[†]**

*Department of Chemistry and Saskatchewan Structural Sciences Centre, University of Saskatchewan, 110 Science Place, Saskatoon, Saskatchewan S7N 5C9, Canada*

Received September 20, 2005

The synthesis, characterization, structure, and electrochemistry of [1.1]ferrocenophanes, bridged by the heavier group 13 elements aluminum (**1a**), gallium (**1b**), and indium (**1c**), are described and discussed. Compounds **1a**–**c** have been synthesized from dilithioferrocene and intramolecularly coordinated group 13 element dihalides $Ar'EX_2$ ($Ar' = 2\text{-}(Me_2NCH_2)C_6H_4$; $EX_2 = AlCl_2$, $GaCl_2$, $InI_2$). Although the synthesis and characterization of **1a** by single-crystal X-ray analysis has been described recently (Braunschweig, H.; Burschka, C.; Clentsmith, G. K. B.; Kupfer, T.; Radacki, K. *Inorg. Chem.* **2005**, *44*, 4906), compounds **1b** and **1c** are described for the first time. The galla (**1b**) and the inda (**1c**) [1.1]ferrocenophane have been characterized by single-crystal X-ray determination [**1b**: $C_{38}H_{40}Fe_2Ga_2N_2$, monoclinic, $P2_1/c$, $a = 10.3467(5)$ Å, $b = 11.6311(4)$ Å, $c = 14.0747(7)$ Å, $\beta = 105.931(2)°$, $Z = 2$; **1c**: $C_{38}H_{40}Fe_2In_2N_2$, monoclinic, $P2_1/c$, $a = 10.5522(7)$ Å, $b = 11.8476(8)$ Å, $c = 13.9855(9)$ Å, $\beta = 104.990(3)°$, $Z = 2$]. All three compounds **1a**–**c** are anti conformers with trans orientations of the two donating $NMe_2$ groups. For the [1.1]ferrocenophane **1a**, an unprecedented fully reversible two-electron redox process was observed by cyclic voltammetry, whereas the corresponding Ga and In species exhibit a more conventional stepwise redox chemistry. According to the Robin–Day classification, **1a** is a class I and **1b** and **1c** are class II species. In addition to the reversible processes, compound **1a** shows an irreversible oxidation at higher voltages accompanied by adsorption processes. The irreversible adsorption process was investigated with an electrochemical quartz crystal microbalance (EQCM).

## Introduction

During the last two decades, inorganic polymers containing metals in their backbones have attracted considerable interest because of their wide range of tunable properties (e.g., redox, magnetic, electrical, and chemical). The main route to these polymers is via ring-opening polymerization (ROP) of strained [1]ferrocenophanes (Figure 1, **I**) developed by Manners and co-workers.[1] The formal dimer of a [1]-ferrocenophane is an unstrained [1.1]ferrocenophane, where two ferrocene moieties are linked by two $ER_x$ groups (Figure 1, **II**).

To date, [1.1]ferrocenophanes with various R groups have been reported for elements of groups 13 (B, Al, Ga),[2−4] 14 (C, Si, Sn, Pb),[5−8] and 15 (P).[9] The conformation of a dimer largely depends on the size of the bridging element E and the bulkiness of the substituents R. All reported group 13 bridged [1.1]ferrocenophanes adopt an anti conformation. Although not useable for ROP, because of the lack of intrinsic ring strain, [1.1]ferrocenophanes have attracted

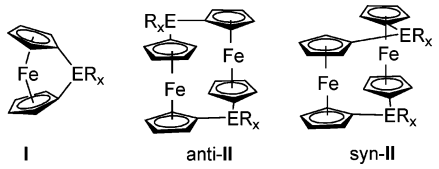


**Figure 1.** $ER_x$-bridged ferrocenophanes. [1]Ferrocenophanes (**I**) and the two conformations of [1.1]ferrocenophanes (**II**).

* To whom correspondence should be addressed. E-mail: jens.mueller@usask.ca.
[†] Department of Chemistry.
[§] Saskatchewan Structural Sciences Center.

(1) (a) Nguyen, P.; Gomez-Elipe, P.; Manners, I. *Chem. Rev.* **1999**, *99*, 1515. (b) Manners, I. *Chem. Commun.* **1999**, 857. (c) Manners, I. *Science* **2001**, *294*, 1664.
(2) Scheibitz, M.; Winter, R. F.; Bolte, M.; Lerner, H.-W.; Wagner, M. *Angew. Chem., Int. Ed.* **2003**, *42*, 924.
(3) (a) Schachner, J. A.; Lund, C. L.; Quail, J. W.; Müller, J. *Acta Crystallogr.* **2005**, *E61*, m682. (b) Braunschweig, H.; Burschka, C.; Clentsmith, G. K. B.; Kupfer, T.; Radacki, K. *Inorg. Chem.* **2005**, *44*, 4906.



10.1021/ic051616y CCC: $33.50 
Published on Web 11/10/2005

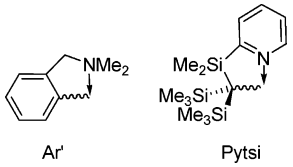


**Figure 2.** Intramolecularly coordinating ligands.

significant interest for different reasons. The methylene-bridged *syn*-[1.1]ferrocenophane ($ER_x = CH_2$) catalyzes the formation of $H_2$ upon protonation.[10] Furthermore, the deprotonation of the *syn*-[1.1]ferrocenophane resulted in a carbanion with an unprecedented hydrogen bond between the two bridging carbon atoms.[10]

The electronic interaction between the two ferrocene redox centers in [1.1]ferrocenophanes can be classified according to the Robin−Day scheme.[11] In class I compounds, no interaction between the redox centers exists, and thus the molecule displays the properties of the isolated redox centers. For classes II and III, the two redox centers influence each other, which is noticeable in the redox properties and spectroscopic properties of the dimer. For class II systems, the interactions are moderate interactions, whereas for class III systems, the redox centers interact strongly.[11] At present, all of the reported [1.1]ferrocenophanes display two fully reversible one-electron oxidation waves. This is generally interpreted by the sequential oxidation of the two iron centers, initially generating a monocation, which in a separate step is oxidized at a higher oxidation potential to generate a dicationic species. In general, [1.1]ferrocenophanes are classified as class II compounds exhibiting moderate electronic interactions between the two redox centers.

In the course of our investigation of ferrocenophanes equipped with the heavier group 13 elements Al, Ga, and In, we employed two different intramolecularly coordinating ligands (Figure 2). The "pytrisyl" ligand is derived from the parent trisyl ligand $C(SiMe_3)_3$ by formal substitution of one methyl group with a pyridyl ring. This bulky ligand with donor capability was introduced by Eaborn and Smith in 2000.[12] Recently, we have shown that reaction of dilithioferrocene with (Pytsi)$ECl_2$ (E = Al,[13] Ga[14]) gives access to

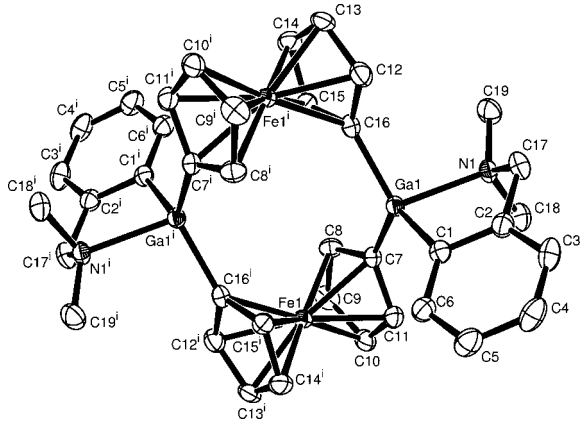


**Figure 3.** ORTEP plot of compound **1b**. Thermal ellipsoids are drawn at the 50% probability level. H atoms are omitted for clarity. $X^i$ atoms are generated by $-x, -y, -z$ operation.

[1]ferrocenophanes, the first [1]metallocenophanes with aluminum and gallium in the bridging position. In the case of the indium compound (Pytsi)$InCl_2$, an unusual ferrocenophane with an In−($\mu$-Cl)$_2$−In moiety was characterized.[14]

Within this report, we describe the synthesis and electrochemical analysis of [1.1]ferrocenophanes with bridging elements Al, Ga, and In (Figure 1). As the ligand R attached to the group 13 element, we used the intramolecularly coordinating "one-armed" phenyl substituents, 2-($Me_2NCH_2$)-$C_6H_4$ (Ar′, Figure 2).

## Results and Discussion

Reaction of dilithioferrocene with Ar′$EX_2$ (Ar′ = 2-($Me_2$-$NCH_2$)$C_6H_4$; $EX_2$ = $AlCl_2$, $GaCl_2$, $InI_2$) gave the respective [1.1]ferrocenophanes in moderate yields (eq 1).

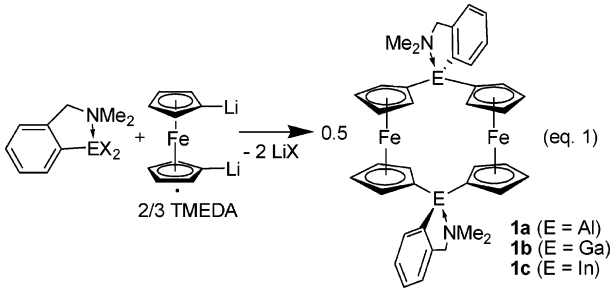


In the course of our investigations, the synthesis and molecular structure of the [1.1]ferrocenophane **1a** have been published by Braunschweig et al.[3b] Their published data agree very well with ours, including that of a structure determination by a single-crystal X-ray analysis. The molecular structures of compounds **1b** and **1c** are depicted in Figures 3 and 4; the crystal and structural refinement data are compiled in Table 1. All three [1.1]ferrocenophanes **1a**−**c**[3b] are isostructural and anti conformers (Figure 1). In addition

(4) (a) Uhl, W.; Hahn, I.; Jantschak, A.; Spies, T. *J. Organomet. Chem.* **2001**, *637*, 300. (b) Jutzi, P.; Lenze, N.; Neumann, B.; Stammler, H. G. *Angew. Chem., Int. Ed.* **2001**, *40*, 1424. (c) Althoff, A.; Jutzi, P.; Lenze, N.; Neumann, B.; Stammler, A.; Stammler, H.-G. *Organometallics* **2002**, *21*, 3018. (d) Althoff, A.; Jutzi, P.; Lenze, N.; Neumann, B.; Stammler, A.; Stammler, H. G. *Organometallics* **2003**, *22*, 2766.
(5) (a) Watts, W. E. *J. Am. Chem. Soc.* **1966**, *88*, 855. (b) Watts, W. E. *J. Organomet. Chem.* **1967**, *10*, 191.
(6) (a) Berenbaum, A.; Lough, A. J.; Manners, I. *Organometallics* **2002**, *21*, 4415. (b) Calleja, G.; Carré, F.; Cerveau, G.; Labbé, P.; Coche-Guérente, L. *Organometallics* **2001**, *20*, 4211. (c) Zechel, D. L.; Foucher, D. A.; Pudelski, J. K.; Yap, G. P. A.; Rheingold, A. L.; Manners, I. *J. Chem. Soc., Dalton Trans.* **1995**, 1893. (d) Park, J.; Seo, Y.; Cho, S.; Whang, D.; Kim, K.; Chang, T. *J. Organomet. Chem.* **1995**, *489*, 23.
(7) (a) Rulkens, R.; Lough, A. J.; Manners, I. *Angew. Chem., Int. Ed.* **1996**, *35*, 1805. (b) Jaekle, F.; Rulkens, R.; Zech, G.; Foucher, D. A.; Lough, A. J.; Manners, I. *Chem.—Eur. J.* **1998**, *4*, 2117.
(8) Utri, G.; Schwarzhans, K.-E.; Allmaier, G. M. *Z. Naturforsch. B* **1990**, *45*, 755.
(9) Brunner, H.; Klankermayer, J.; Zabel, M. *J. Organomet. Chem.* **2000**, *601*, 211.
(10) Mueller-Westerhoff, U. T. *Angew. Chem., Int. Ed.* **1986**, *25*, 702.
(11) Robin, M. B.; Day, P. *Adv. Inorg. Chem. Radiochem.* **1967**, *10*, 247.
(12) Al-Juaid, S. S.; Eaborn, C.; Hitchcock, P. B.; Hill, M. S.; Smith, J. D. *Organometallics* **2000**, *19*, 3224.
(13) Schachner, J. A.; Lund, C. L.; Quail, J. W.; Müller, J. *Organometallics* **2005**, *24*, 785.
(14) Schachner, J. A.; Lund, C. L.; Quail, J. W.; Müller, J. *Organometallics* **2005**, *24*, 4483.

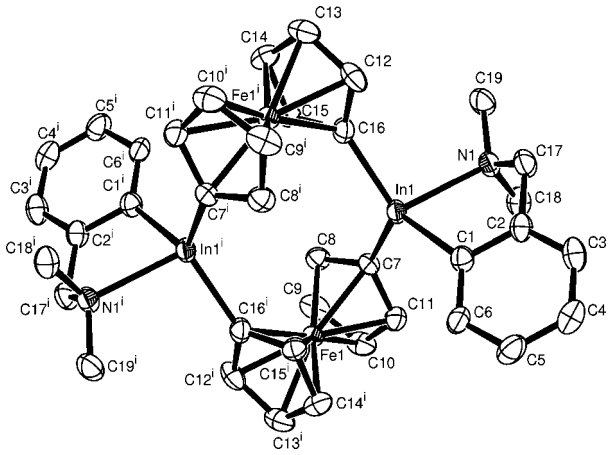


**Figure 4.** ORTEP plot of compound **1c**. Thermal ellipsoids are drawn at the 50% probability level. H atoms are omitted for clarity. $X^i$ atoms are generated by $-x, -y, -z$ operation.

to the relative orientation of the bridging elements, which is described by the prefixes anti and syn (see Figure 1), the dimethyl amino groups, in principle, could exhibit two different orientations each. For all three species **1a**−**c**, the amino moieties are pointing away from each other. The two amino groups are trans oriented; they are outside the space provided by the two ferrocene units.

Like those in **1a**, the E−C and E−N bond lengths and the angles around the metal centers of **1b** and **1c** are unremarkable (**1a**:[3b] Al−N = 2.0748(14) Å; Al−C = 1.9571(16), 1.9599(17), 1.9856(17) Å. **1b**: Ga1−N1 = 2.178(3) Å; Ga−C1, −C7, −C16 = 1.988(3), 1.951(4), 1.963(3) Å; ∠C1−Ga1−C16 = 123.20(15)°; C7−Ga1−C16 = 117.71(15)°; C1−Ga1−C7 = 115.37(15)°. **1c**: In1−N1 = 2.386(4) Å; In1−C1, −C7, −C16 = 2.178(5), 2.150(5), 2.136(5) Å; ∠C1−In1−C16 = 126.03(18)°; C7−In1−C16 = 116.32(17)°; C1−In1−C7 = 115.63(17)°). With respect to a possible Fe−Fe interaction in these species, the Fe−Fe distances are worth mentioning. As expected, the Al compound **1a** (5.443 Å)[3b] and the Ga species **1b** (5.462 Å) exhibit a similar Fe−Fe distance, whereas that of **1c** is slightly longer (5.724 Å).

$^1$H and $^{13}$C NMR spectra of compounds **1a**−**c** show signal patterns for one type of Ar′ and one type of $C_5H_4$ ligand. These spectra can be interpreted as being caused by time-averaged $C_{2h}$ symmetrical species. This indicates that the molecular structures of **1a**−**c** in solution are similar to those in the solid state, taking into account the well-known, fast inversion of the five-membered rings of the coordinated Ar′ ligands.[15]

We expected to find that compounds **1a**−**c** exhibit essentially the same electrochemistry and display weak electronic communication between the redox centers (class II compounds). However, to our surprise, the redox properties examined by cyclic voltammetry (CV) of the Al, Ga, and In species are significantly different. The redox properties of compounds **1a**−**c** are summarized in Table 2.

The CV of the Al species **1a** shows two oxidation waves and one reduction wave (Figure 5). The first redox wave ($E_{1/2}$ = 0.36 V vs Ag/AgCl) is fully reversible, and corresponds to a two-electron process. To calculate the number of electrons involved in the oxidation step, we measured the Cottrell constant via chronocoulometry on a Pt electrode by assuming the same diffusion coefficient as that measured for **1b** ($D = 2.4 \times 10^{-5}$ cm$^2$/s, assuming $n$ = 2e$^-$).[16] The gallium compound **1b** displays two reversible one-electron processes at $E_{1/2}$ = 0.05 and 0.35 V (Figure 6). However, the redox behavior of the In compound **1c** is more complex (Figure 7, Table 2). Because the half-wave potentials $E_{1/2}$ could not be obtained reliably, we would like to report the oxidation potentials $E_{ox}$ for **1c** instead. The voltammogram is composed of two major oxidation waves at $E_{ox1}$ = 0.12 V and $E_{ox2}$ = 0.39 V and two poorly resolved minor oxidation waves around $E'_{ox1}$ = 0.0 V and $E'_{ox2}$ = 0.2 V (Figure 7, Table 2). Importantly, the redox waves of all species are fully reversible, and have a ratio of the peak currents that is close to unity.

Compound **1a** displays the redox chemistry of isolated Fe centers lacking any electronic communication, thus belonging to class I, according to the Robin−Day classification.[11] To the best of our knowledge, this is an unprecedented behavior for [1.1]ferrocenophanes. In contrast, the Ga species **1b** displays the expected stepwise oxidation, showing moderate electronic interaction between the two ferrocene moieties. The separation between the oxidation potentials in **1b** $\Delta E_{ox}$ is 0.30 V, from which an exchange constant of $K_c$ = 118 000 was obtained,[17] indicating class II behavior. The two major and two minor oxidation waves for the In compound **1c** hint at the presence of two different species in solution (Figure 7). It is feasible that compound **1c** consists of a mixture of two isomers that can be differentiated in solution by CV. This speculation is supported by the fact that at −80 °C in $C_7D_8$, a second set of signals emerges in the $^1$H NMR spectra of **1c**. We assume that the major redox waves belong to an isomer with a structure similar to that found for **1c** in the crystal lattice. We do not have experimental evidence about the nature of the minor species; however, the NMR spectrum of **1c** at room temperature reveals only one species, as it shows only one set of signals.

In addition to the reversible two-electron wave, compound **1a** displays a second but irreversible oxidation process at 1.2 V (Figure 5). Furthermore, we observed a white precipitate that was produced during extensive cycling, which prompted us to carry out studies with an electrochemical quartz crystal microbalance (EQCM). It can be seen in Figure 8 that the Al dimer **1a** showed significant adsorption to the gold electrode, corresponding to an increase in mass on the quartz crystal starting around 1.0 V (Figure 5 and Figure 8b).

When the sweep was reversed at 0.9 V, compound **1a** showed full redox reversibility without any adsorption to the electrode. To obtain some information about the deposited

(15) Müller, J.; Englert, U. *Chem. Ber.* **1995**, *128*, 493.

(16) Cottrell constant: $it^{1/2} = 1.77nFAD^{1/2}C^*$, where $n$ is the number of electrons transferred, $F$ is the Faraday constant, $A$ is the area of the electrode, $D$ is the diffusion coefficient, and $C^*$ is the bulk concentration of the electrochemical reactant.

(17) Creutz, C. *Prog. Inorg. Chem.* **1983**, *30*, 1.

**Table 1.** Crystal and Structural Refinement Data for Compounds **1b** and **1c**

| | **1b** | **1c** |
|---|---|---|
| empirical formula | $C_{38}H_{40}Fe_2Ga_2N_2$ | $C_{38}H_{40}Fe_2In_2N_2$ |
| fw | 775.85 | 866.06 |
| wavelength (Å) | 0.71073 | 0.71073 |
| cryst syst | monoclinic | monoclinic |
| space group (No.) | $P2_1/c$ | $P2_1/c$ |
| $Z$ | 2 | 2 |
| $a$ (Å) | 10.3467(5) | 10.5522(7) |
| $b$ (Å) | 11.6311(4) | 11.8476(8) |
| $c$ (Å) | 14.0747(7) | 13.9855(9) |
| α (deg) | 90 | 90 |
| $\beta$ (deg) | 105.931(2) | 104.990(3) |
| $\gamma$ (deg) | 90 | 90 |
| vol (Å$^3$) | 1628.75(13) | 1688.94(19) |
| $d_{calc}$ (mg/m$^3$) | 1.582 | 1.703 |
| $T$ (K) | 173(2) | 173(2) |
| abs coeff (mm$^{-1}$) | 2.540 | 2.219 |
| $\theta$ range (deg) | 2.69−26.37 | 3.02−25.98 |
| no. of reflns collected | 6339 | 19 945 |
| no. of ind. reflns | 3325 [$R$(int) = 0.0520] | 3304 [$R$(int) = 0.0891] |
| abs corrn | none | $\psi$ scan, $T_{min}$ = 0.269, $T_{max}$ = 0.350 |
| ref method | full-matrix least-squares on $F^2$ | |
| data/restr/params | 3325/0/201 | 3304/0/201 |
| GOF on $F^2$ | 1.021 | 1.086 |
| final R indices [$I > 2\sigma(I)$] | R1 = 0.0394, wR2 = 0.0711 | R1 = 0.0448, wR2 = 0.1019 |
| R indices (all data) | R1 = 0.0708, wR2 = 0.0817 | R1 = 0.0560, wR2 = 0.1107 |
| largest diff. peak and hole (e Å$^{-3}$) | 0.563 and −0.528 | 2.056 and −1.635 |

**Table 2.** Oxidation Potentials and Classification of the Three [1.1]Ferrocenophanes Studied[a]

| | $E_{1/2}$ (V) | | $E_{ox1}$ (V) | $E_{ox2}$ (V) | Robin−Day class |
|---|---|---|---|---|---|
| **1a** | 0.36 | | 0.54 | | I |
| **1b** | 0.05 | 0.35 | 0.11 | 0.41 | II |
| **1c**[a] | [b] | [b] | 0.12 (0.0) | 0.39 (0.2) | II |

[a] Values in parentheses for **1c** correspond to the two minor oxidation waves. [b] $E_{1/2}$ could not be reliably determined for **1c**.

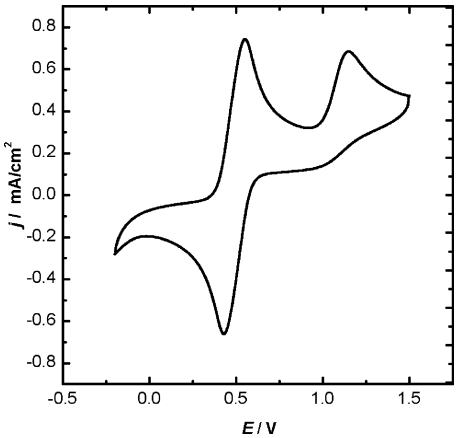


**Figure 5.** Cyclic voltammogram of compound **1a**.

material, we analyzed the topography of the gold electrode by atomic force microscopy (AFM, see the Supporting Information) and the elemental composition by X-ray photoelectron spectroscopy (XPS) and Auger electron spectroscopy (AES). For the AFM measurement, we examined samples for which a constant potential of 1.3 V for 5, 15, and 30 min had been applied. After 30 min, the current leveled out to zero, indicating that the surface of the electrode was completely covered, corresponding to a total deposition of a few hundred nanograms. After 5 min, an islandlike growth of deposited material on the surface was observed by AFM. After 15 min, the gold surface was largely covered,

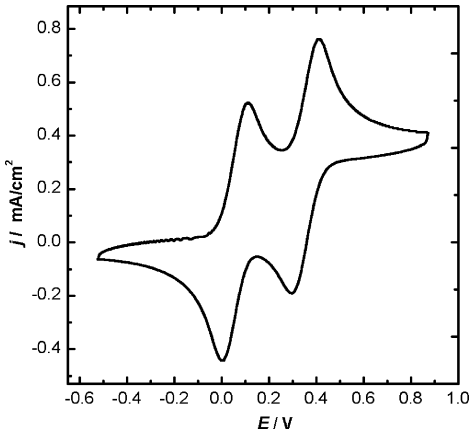


**Figure 6.** Cyclic voltammogram of compound **1b**.

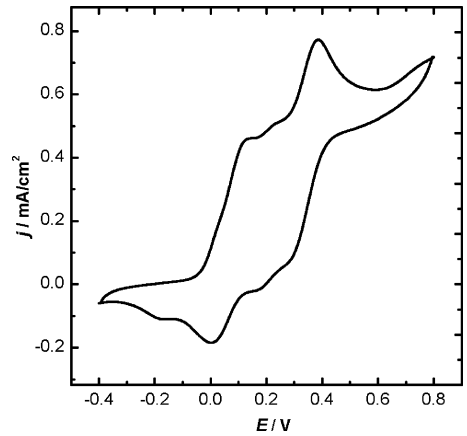


**Figure 7.** Cyclic voltammogram of compound **1c**.

and after 30 min the surface was completely covered with multiple layers of material.

From XPS and AES, the five most abundant elements of the deposited material were C, O, Fe, Al, and N. It is fair to assume that oxygen was introduced through an exposure of

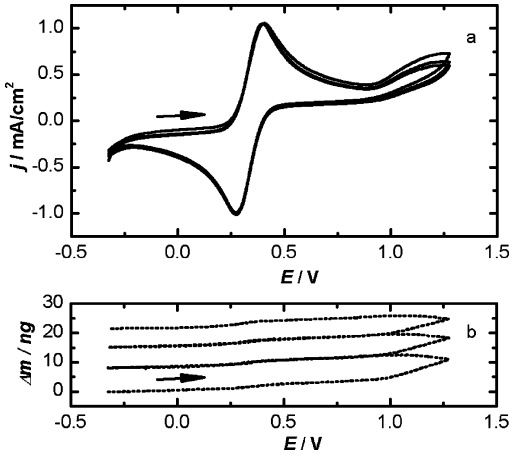


**Figure 8.** (a) Cyclic voltammogram of compound **1a** (gold disk on quartz crystal as a working electrode). (b) QCM response. Significant increase in mass (~10 ng) starting around 1.0 V indicates deposition of **1a** onto the electrode.

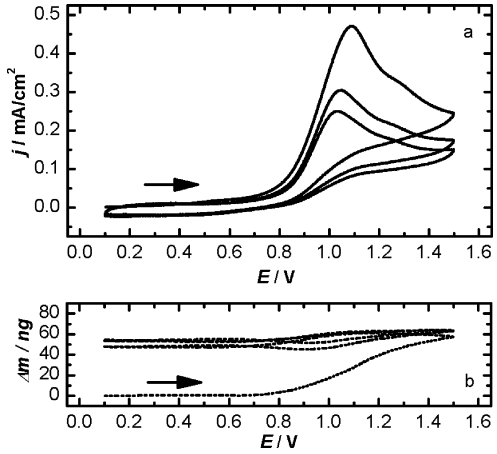


**Figure 9.** (a) Cyclic voltammogram of $Ar'AlMe_2$. (b) QCM response. Large increase in mass (~50 ng) starting around 0.8 V indicates a deposition process.

the sample to air after deposition. With respect to the four elements C, Fe, Al, and N, the elemental composition found for the deposited material reflects the overall composition of the initial ferrocenophane **1a** (see Experimental Section).

Because the two ferrocene moieties in **1a** are already oxidized at the same potential ($E_{1/2}$ = 0.36 V and $E_{ox1}$ = 0.54 V), the occurrence of the second irreversible oxidation at 1.2 V must be due to an oxidation somewhere else in **1a**. Aluminum alkyl species exhibit highly polar Al−C bonds, and are known to be reducing agents. We assume that at higher voltage, C atoms bound to aluminum become oxidized, which must result in a breakage of the respective Al−C bond, obviously an irreversible process. To test this hypothesis, we recorded an EQCM of $Ar'AlMe_2$ (Figure 9). This compound serves as a ferrocene-free model for **1a**, because it shows aluminum with a first-coordination sphere similar to that in **1a**.

The model compound $Ar'AlMe_2$ displays an irreversible oxidation wave similar to that of **1a**, at a comparable potential and with an even larger adsorption to the electrode. The first sweep already deposited more than 50 ng of material, which almost completely covered the electrode disk. Deposited material withstood multiple washings with various solvents, and is rather soft.

## Conclusion

Heavier group 13 element-containing compounds equipped with the intramolecularly coordinating one-armed phenyl ligand Ar′ (Figure 2) give access to the [1.1]ferrocenophanes **1a**−**c**. Although the aluminum species **1a** was published very recently,[3b] and the gallium compound **1b** is another example of a [1.1]digallaferrocenophane,[4] **1c** is the first indium-bridged [1.1]ferrocenophane. In the solid state, **1a**−**c** display the expected anti conformation. Interestingly, similar reactions with pytrisyl-containing starting compounds yielded strained [1]ferrocenophanes (Pytsi, Figure 2).[13,14]

The three isostructural [1.1]ferrocenophanes **1a**−**c** display distinctively different electrochemical behavior, as revealed by cyclic voltammetry. Only the [1.1]digallaferrocenophane **1b** shows the expected voltagramm, with two separated, fully reversible one-electron oxidation steps. The [1.1]dialuminaferrocenophane **1a** shows a fully reversible two-electron oxidation step. Furthermore, at a higher potential, it shows an irreversible oxidation step, which is accompanied by adsorption processes on the gold electrode. On the other hand, the [1.1]diindaferrocenophane **1c** exhibits a more complex cyclic voltagramm, with four reversible oxidation steps. We attribute this to the presence of conformational isomers in solution. To the best of our knowledge, the Al species **1a** is the first [1.1]ferrocenophane in which the two Fe atoms act independently (class I). So far, the reasons for this exceptional behavior remain unclear. Further investigations to illuminate the origins of the different properties of Al-bridged ferrocenophanes compared to those of Ga-bridged ferrocenophanes are currently underway.

## Experimental Section

**Electrochemistry.** All experiments were conducted with a CH Instruments, Inc., model 660B electrochemical analyzer. A gold working electrode (BAS, 2 mm) was employed. The quasi-reference electrode was a silver wire immersed in 0.1 M tetrabutylammonium hexafluorophosphate (TBAPF) in EtOH solution separated by a Vycor tip (the potential of which is 75 mV vs a standard hydrogen electrode (SHE)). Platinum wire was used as the auxiliary electrode. In each case, IR compensation was applied. Solutions of **1a**−**c** (1 mM) were prepared in dry dichloromethane with 0.1 M TBAPF as supporting electrolyte. The scan rate for all CVs reported was 100 mV/s. Experiments were conducted under strict inert conditions to exclude interactions with oxygen and moisture (glovebox, vacuum pump, and nitrogen purging). All measurements were carried out in a nitrogen-purged electrochemical cell (see the Supporting Information). Measurements were taken at room temperature (22 °C).

EQCM experiments were conducted with a CH Instruments, Inc., model CHI 440 EQCM instrument. An 8 MHz quartz crystal covered with 100 Å of Ti and 1000 Å of Au was used as a working electrode (commercially available from CH Instruments). The gold electrode area was 0.205 $cm^2$.

**Synthesis.** All manipulations were carried out using standard Schlenk techniques. Solvents were dried using a Braun Solvent Purification System, and were stored under argon over a 4 Å molecular sieve. $C_6D_6$ and $C_7D_8$ were degassed prior to use, and

were stored under argon over a 4 Å molecular sieve. $GaCl_3$ (99.99%, Aldrich) and $InI_3$ (99.999%, Alpha Aesar) were purchased and used as received. $^1H$ and $^{13}C$ NMR spectra were recorded on a Bruker 500 MHz Avance spectrometer; chemical shifts were referenced to the residual protons of the deuterated solvent. All NMR spectra are in $C_6D_6$ at 25 °C, unless noted differently. Mass spectra were measured on a VG 70SE mass spectrometer, and were reported in the form *M* (%*I*) [F], where *M* is the mass observed, %*I* is the intensity of the peak relative to the most intense peak in the spectrum, and F is the molecular ion or fragment. Only ions with intensities greater than 10% are listed. Elemental analysis was performed on a Perkin-Elmer 2400 CHN Elemental Analyzer; samples were prepared in a glovebox, and $V_2O_5$ was added to promote combustion.

The compounds $Ar'AlCl_2$,[15] $Ar'Me_2$,[15] $Ar'GaCl_2$,[18] and $Ar'InI_2$[19] were synthesized according to literature procedures ($Ar' = 2\text{-}(Me_2NCH_2)C_6H_4$). In the course of our investigations, the synthesis and characterization of **1a** was published;[3b] the synthetic procedure we used for compound **1a** is described in the Supporting Information.

**Synthesis of 1b.** A solution of $Ar'GaCl_2$ (1.025 g, 3.73 mmol) in toluene (30 mL) was chilled to −10 °C, and was added dropwise via tubing to a chilled (−10 °C) suspension of dilithioferrocene·$^2/_3$TMEDA (1.027 g, 3.73 mmol) in toluene (30 mL). After being stirred for 16 h, the solution changed in color to red. After being filtered, the solution was concentrated by evacuation until crystallization started. To promote crystallization, we cooled the solution to 6 °C (0.215 g, 0.28 mmol, 15%). $^1H$ NMR (500 MHz): $\delta$ 1.70 (s, 12H, $NMe_2$), 3.24 (s, 4H, $-CH_2-$), 3.99, 4.37, 4.48, 5.07 (pst, 16H, $C_5H_4$), 6.99 (d, 2H, $C_6H_4$), 7.28 (pst, 2H, $C_6H_4$), 7.42 (pst, 2H, $C_6H_4$), 8.45 (d, 2H, $C_6H_4$). $^{13}C$ NMR (125.8 MHz): $\delta$ 45.61 ($NMe_2$), 66.40 ($-CH_2-$), 70.91 (*ipso*-C, $C_5H_4$), 70.76, 71.05, 74.79, 75.20 ($C_5H_4$), 124.99, 127.42, 127.59, 130.08, 144.59, 150.99 ($C_6H_4$). Anal. Calcd for $C_{38}H_{40}Fe_2Ga_2N_2$ (775.87): C, 58.82; H, 5.20; N, 3.61. Found: C, 59.62; H, 5.35; N, 3.80. MS (70 eV, EI+) *m*/*z* (%): 776 (100) [$M^+$], 571 (5.6) [$M^+ - Ar'Ga$], 388 (14) [$^1/_2M^+ + H$].

**Synthesis of 1c.** $Ar'InI_2$ (0.880 g, 1.75 mmol) was dissolved in THF (15 mL), chilled to −10 °C, and added dropwise via tubing to a chilled (−10 °C) suspension of dilithioferrocene·$^2/_3$TMEDA (0.482 g, 1.75 mmol) in THF (15 mL). After being stirred for 16 h, the solution changed in color to red. The solvent was removed under high vacuum, to give a sticky orange-brown solid. This solid was redissolved in benzene (20 mL), and was filtered. At 6 °C, orange crystals of **1c** precipitated (0.440 g, 0.51 mmol, 58%). $^1H$ NMR (500 MHz): $\delta$ 1.81 (s, 12H, $NMe_2$), 3.24 (s, 4H, $-CH_2-$), 4.04, 4.45, 4.53, 4.97 (pst, 16H, $C_5H_4$), 7.01 (d, 2H, $C_6H_4$), 7.25 (pst, 2H, $C_6H_4$), 7.35 (pst, 2H, $C_6H_4$), 8.37 (d, 2H, $C_6H_4$). $^{13}C$ NMR (125.8 MHz): $\delta$ 45.38 ($NMe_2$), 67.55 ($-CH_2-$), 68.30 (*ipso*-C, $C_5H_4$), 71.30, 71.64, 75.44, 76.35 ($C_5H_4$), 126.35, 127.37, 127.75, 139.11, 145.37, 155.71 ($C_6H_4$). Anal. Calcd for $C_{38}H_{40}Fe_2In_2N_2$ (866.06): C, 52.70; H, 4.66; N, 3.23. Found: C, 50.06; H, 4.75; N, 3.10. MS (70 eV, EI+) *m*/*z* (%): 866 (100) [$M^+$], 619 (7.3) [$M^+ - Ar'In$], 433 (14) [$^1/_2M^+$], 383 (23) [$Ar'_2In^+$], 115 (37) [$In^+$].

**X-ray Structural Analysis for 1b and 1c.** Data were collected at −100 °C on a Nonius Kappa CCD diffractometer, using the COLLECT program.[20] Cell refinement and data reductions used the programs DENZO and SCALEPACK.[21] The program SIR97[22] was used to solve the structure, and SHELXL97[23] was used to refine the structure. All H atoms were placed in calculated positions, with C−H distances in the range 0.95−0.99 Å, and were included in a riding model approximation. $U_{iso}$(H) was constrained to be 1.2 $U_{eq}$(C) for all aromatic protons and 1.5 $U_{eq}$(C) for all methyl protons.

**Surface Analysis.** X-ray photoelectron spectroscopy (XPS) and Auger electron spectroscopy (AES) were done at the Alberta Center for Surface Engineering and Science (ACSES) using a Kratos Axis 165 spectrometer. Several spots of the sample were analyzed by XPS, and all spectra showed C, O, and Fe as the three elements with the highest mass concentrations. A representative analysis (aperture of 120 $\mu$m) for just five elements (set to 100%) gave C (1s, 50.6%), O (1s, 24.7%), Fe (2p, 17.9%), Al (2p, 5.0%), N (1s, 1.8%); if only four elements (set to 100%) are used, the results are C (1s, 67.2%), Fe (2p, 23.7%), Al (2p, 6.6%), N (1s, 2.4%). Several different positions of the sample previously analyzed by XPS were analyzed by AES. Representative results for three different positions are C (70.5, 71.0, 68.1%), O (13.3, 12.8, 15.2%), Fe (10.6, 9.7, 9.3%), Al (3.4, 4.5, 5.5%), N (2.2, 2.0, 1.8%); if only four elements (set to 100%) are used, the results are C (80.7, 81.4, 80.3%), Fe (12.2, 11.1, 11.0%), Al (3.9, 5.2, 6.5%), N (2.5, 2.3, 2.1%). The results from XPS and AES compare well with the mass concentrations of the four elements C, Fe, Al, and N in **1a** (set to 100%): C (70.21%), Fe (17.18%), Al (8.30%), N (4.31%).

**Acknowledgment.** We thank the Natural Sciences and Engineering Research Council of Canada (NSERC Discovery Grant), the Department of Chemistry, and the University of Saskatchewan for their generous support. We thank the Canada Foundation for Innovation (CFI) and the government of Saskatchewan for funding of the X-ray and NMR facilities in the Saskatchewan Structural Sciences Centre (SSSC). We thank Dr. D. Karpuzov of the Alberta Center for Surface Engineering and Science (ACSES) for obtaining the XPS and AES data. H.-B.K. is the Canada Research Chair in Biomaterials.

**Supporting Information Available:** Text detailing the synthesis and characterization of compound **1a**, crystallographic data for **1b** and **1c** in CIF file format, picture of the electrochemical cell, and AFM images of adsorbed material. This material is available free of charge via the Internet at http://pubs.acs.org.

IC051616Y

(18) Brown, D. S.; Decken, A.; Cowley, A. H. *J. Am. Chem. Soc.* **1995**, *117*, 5421.
(19) Gabbaie, F. P.; Isom, H. S.; Decken, A.; Culp, R. D.; Cowley, A. H. *Main Group Chem.* **1995**, *1*, 9.
(20) *COLLECT*; Enraf-Nonius BV: Delft, The Netherlands, 1998.
(21) Otwinowski, Z.; Minor, W. In *Macromolecular Crystallography, Part A*; Carter, C. W., Sweet, R. M., Eds.; Academic Press: London, 1997; Vol. 276, pp 307−326.
(22) Altomare, A.; Burla, M. C.; Camalli, M.; Cascarano, G.; Giacovazzo, C.; Guagliardi, A.; Moliterni, A. G. G.; Polidori, G.; Spagna, R. *J. Appl. Crystallogr.* **1999**, *32*, 115.
(23) Sheldrick, G. M. *SHELXS97* and *SHELXL97*; University of Göttingen: Göttingen, Germany, 1997.